6

Biosensing Based on Luminescent Semiconductor Quantum Dots and Rare Earth Up-conversion Nanoparticles

Jun Zhang[1,2], Changyan Li[1,2], Wenzhi Zhao[1,2],
Baocang Liu[1], Yunxia Liu[1] and Gaole Aletan[2]
[1]*College of Chemistry and Chemical Engineering,*
[2]*College of Life Science,*
Inner Mongolia University, Hohhot 010021,
P. R. China

1. Introduction

A biosensor is a device incorporating a biological sensing element either intimately connected to or integrated within a transducer, which is mainly determined by specific molecular recognition such as enzyme-substrate, antibody-antigen and so on. Currently, with the development of nanoscience and nanotechnology, more and more interest has been focused on using nanoparticles to fabricate biosensors (Alivisatos, 2004; Katz, 2004; Rosi 2005). Several kinds of biological sensors based on semiconductor quantum dots (QDs), gold nanoparticles (GNPs), carbon nanotubes (CNTs), fullerene, dendrimer nanoparticles have been presented. Semiconductor QDs are a new class of fluorescent materials for biosensor. In comparison with conventional organic dyes and fluorescent proteins, they have unique optoelectronic properties with size-tunable light emission, superior signal brightness, resistance to photobleaching and broad absorption spectra for simultaneous excitation of multiple fluorescence colors (Alivisatos, 1996). However, the use of semiconductor QDs for biosensor application still has some limitations (Jaiswal, 2004), for instance, the potential toxicity of QDs may pose risks to human health and the environment under certain conditions (Derfus, 2004). In addition, the absorption of UV and visible light by biological samples often induces autofluorescence, which interferes with fluorescent signals obtained from exogenous biomarkers. Moreover, if biological samples are prolonged exposure to UV radiation, it would cause the samples photo-damage and mutation.

The drawbacks of QDs in biosensing application have prompted the development of up-converting nanoparticles (UCNs) emerged as another class of new biosensing materials. Usually, UCNs exhibit intense visible or near-infrared light excited by near-infrared light according to the anti-stokes law. The UCNs also show a sharp emission bandwidth, long lifetime, tunable emission, high photostability, low bio-toxicity and good biocompatibility, which are less harmful to biological samples and have greater penetration depth through biological samples than conventional ultraviolet excitation. Moreover, UCNs can be easily coupled to proteins or other biological macromolecular systems and used in a variety of

assay formats (Yen, 2004; Blasse, 1994). This review is composed of four sections, and is intended to summarize the recent advances in luminescent semiconductor QDs and rare earth UCNs for biosensing application. In the first section, the production mechanism, size-dependent luminescence, spectral characteristics, bioconjugation technology and potential biosensing application of semiconductor QDs are comprehensively reviewed; In the second section, the controlled synthesis, characterization, luminescence mechanism, and biosensing application of rare-earth UCNs are systemically introduced; In the third section, the comparative assessment of advantage and limitation of semiconductor QDs and rare earth UCNs in biosensing application are discussed; In the fourth section, the concluding remarks and perspective for semiconductor QDs and rare-earth UCNs in biosensing application are presented.

2. Semiconductor QDs as fluorescent labels for biosensing application

2.1 Concept of semiconductor QDs

Semiconductors have a filled band called the "valence band" and an empty band known as the "conduction band". At nanoscale dimension, the normally collective electronic properties of semiconductors become severely distorted and the electrons tend to follow the "particle in-a-box" model accounting for approximated band structure (Murray, 1993). From a quantum mechanical point of view, when a semiconductor is irradiated with light of photon energy (h_ν) higher than E_g, an electron will be promoted from the valence to the conduction band, leaving a "hole" or "absence of an electron" in the valence band. Thus, this "hole" is assumed to be a "particle" with its particular effective mass and positive charge. The bound state of the electron-hole pair is called an "exciton" (Brus, 1984). The exciton can be considered a hydrogen-like system, and a Bohr approximation of the atom can be used to calculate the spatial separation of the electron–hole pair of the exciton by Eq. (1):

$$r = \frac{\varepsilon h^2}{\pi m_r e^2} \tag{1}$$

where r is the radius of the sphere, defined by the 3-D separation of the electron-hole pair, ε is the dielectric constant of the semiconductor, m_r is the reduced mass of the electron-hole pair, h is Planck's constant, and e is the charge on the electron. For many semiconductors,
the masses of the electron and hole have been determined by ion cyclotron resonance and are generally in the range 0.1-3 m_e (m_e is the mass of the electron). For typical semiconductor dielectric constants, the calculation suggests that the electron-hole pair spatial separation is 1-10 nm for most semiconductors (Gaponenko, 1998).
Because the physical dimensions of a QD can be smaller than the exciton diameter, the QD is a good example of the "particle-in-a-box" calculations of undergraduate physical chemistry. In those calculations, the energies of the particle in the box depend on the size of the box. In the QD, the bandgap energy becomes size-dependent (Alivisatos, 1996; Gaponenko, 1998; Zhang, 1997; Weller, 1993; Murphy, 2002).

2.2 Optical properties of QDs

QDs are nearly spherical semiconductor particles with diameters on the order of 1-10 nm, containing roughly 200-10,000 atoms. When semiconductor QDs are smaller than their

exciton Bohr radii, the quantum confinement and size-dependent effects make QDs have unique optical properties (Fig. 1): (1) single excitation, multi-emission and size-dependent; (2) large stokes shift, narrow and symmetrical fluorescence peak; (3) visible light range fluorescence and resistance to photobleaching; (4) superior signal brightness. In addition, changing QD surface functional groups, luminescent properties and stability are greatly improved and more conducive to the coupling of biological molecules. For conventional dye molecules, their narrow excitation spectrum makes the simultaneous excitation difficult in most cases, and their broad emission spectrum may cause a long tail at red wavelengths; while for semiconductor QDs, the absorbance onset and emission maximum shift to higher energy with the decrease of particle sizes (Alivisatos, 1996). The excitation tracks the absorbance, resulting in a tunable fluorescence that can be excited efficiently at any wavelength shorter than the emission peak, and therefore the characteristic narrow and symmetric spectrum can be realized regardless of the excitation wavelength (Bruchez, 1998).

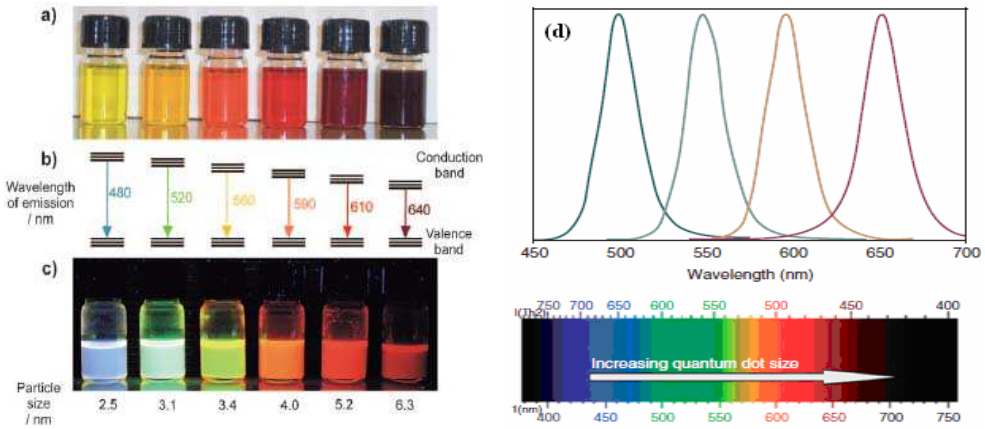

Fig. 1. Size-dependent optical properties of QDs. (a) Surface color of suspensions in toluene in visible light; (b) Schematic diagram of band gap and emission color as a function of particle size; (c) Light emission of suspensions in toluene when excited with UV light; (d) Fluorescence spectra of the QDs samples (from left to right are respectively representative 2.2, 2.9,4.1 and 7.3nm QDs). (Feldmann, 2010; Mansur, 2010; Smith, 2008).

Due to their unique optical properties, semiconductor QDs can be used as fluorescent labels for biological detection. In order to establish the utility of QDs for biological sensing application, mouse 3T3 fibroblast cells were labeled with green and red emitting CdSe/CdS nanocrystals. The green and red labels were spectrally resolved to the eye clearly under the excitation of a single light source by a laser scanning confocal microscope. Nonspecific labeling of the nuclear membrane by both the red and green probes resulted in a yellow color [Fig. 2(a)]. The intensity of the fluorescein drops quickly to autofluorescence levels, whereas the intensity of the QDs drops only slightly. Comparatively, the red QD labels are 20 times as bright, 100 times as stable against photobleaching [Fig. 2(b)] (Bruchez, 1998).
In general, QDs synthesized in nonpolar solutions using aliphatic coordinating ligands are only soluble in nonpolar organic solvents, which are not suit for biological application.

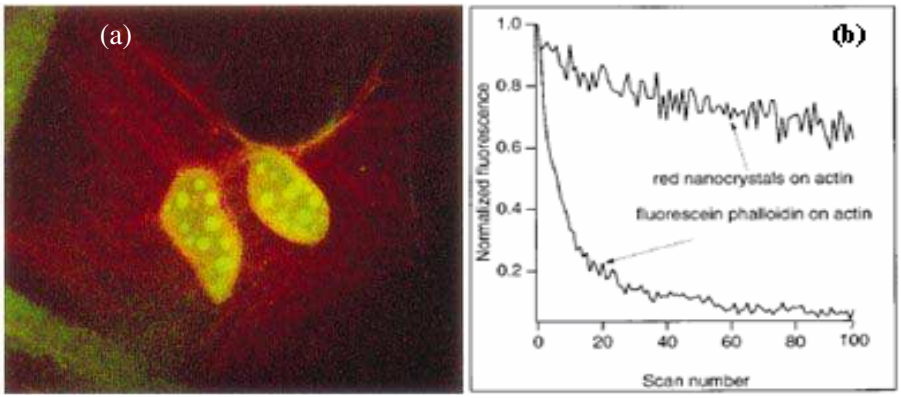

Fig. 2. Schematic diagrams of dual-color labeling and photostability. (a) The mouse 3T3 fibroblasts were labeled with dual color. (b) Sequential scan photostability comparison of fluorescein-phalloidin-labeled actin fibers compared with nanocrystal-labeled actin fibers (Bruchez, 1998).

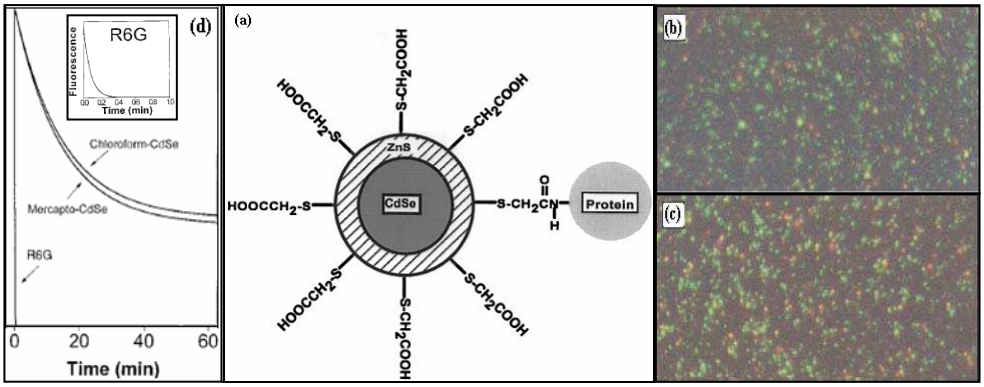

Fig. 3. (a) Scheme of a CdSe/ZnS QD covalently coupled to a protein; (b) Luminescent images obtained from the original QDs; (c) mercapto-solubilized QDs; (d) Time-resolved photobleaching curves for the original QDs, solubilized QDs and dye R6G (Chan, 1998).

Moreover, QDs have a huge surface/volume ratio, which makes them extremely unstable in solution because of the high surface energy. Hence, any route chosen to synthesize QDs should consider the stabilization of the QDs by minimizing the surface energy via "capping" and avoiding further structure growth (Weaver, 2009). Warren and coworkers presented a valuable way to solve this problem by coating CdSe QDs with higher bandgap materials such as ZnS shell in order to increase the photostability and luminescence properties of CdSe QDs (Chan, 1998). When reacting with CdSe/ZnS QDs in chloroform, the mercapto group binds to a Zn atom, and the free carboxyl group is available for covalent coupling to various biomolecules such as proteins by cross-linking to reactive amine groups [Fig. 3(a)] (Hermanson, 1996). A comparison of color luminescence images were obtained from the original QDs, water soluble QDs and protein-conjugated QDs [Figs. 3(b) and (c)], which

indicated that the optical properties of QDs remain unchanged after solubilization and conjugation. The photophysical properties of QD conjugates with rhodamine 6G (R6G) was also studied. The emission of mercapto-CdSe is somehow weaker than that of single QDs, which is nearly 100 times as stable as R6G against photobleaching [Fig. 3(d)].

2.3 Synthesis of biocompatible QDs

The most common method for synthesizing water-soluble QDs is coated with a monolayer of hydrophilic thiols, typically mercaptoacetic acid (MAA), to replace the hydrophobic trioctylphosphine oxide (TOPO) coating on QDs (Chan, 1998; Hood, 2002; Duncan, 2006). But, when the MAA replace the TOPO coating on QDs, the QDs become instable accompanied by significant decreases in the quantum yield to 7% compared with TOPO-coated QDs (Kim, 2004). To overcome this problem, Alivisatos and coworkers developed an effective route to coat QDs with a cross-linked silica shell, which can be readily modified with a variety of organic functionalities such as primary amines, carboxylic acids or thiols (Gerion, 2001). The coated QDs were very stable and retained 60-80% of the quantum yield of the original QDs. Gao and coworkers developed another effective method to synthesize CdSe/ZnS QDs stabilized by a coordinating ligand (TOPO) and an amphiphilic polymer coating through hydrophobic attraction (Gao, 2004). Because of the strong hydrophobic interactions between TOPO and polymer hydrocarbon, the two layers bonds to each other and form a hydrophobic protection structure that resists hydrolysis and enzymatic degradation even under complex *in vivo* conditions. In most designs of the amphiphilic polymers, carboxylic acids provide solubility in water and can be utilized as

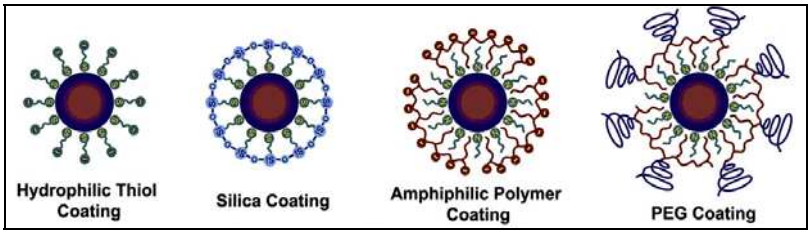

Fig. 4. Schematic diagrams of biocompatible QDs.

chemical handles for conjugation to primary amines in proteins through water soluble cross-linking reagents such as 1-ethyl-3-(3-dimethylaminopropyl) carbodiimide (EDAC). Similarly, many of these QDs also may be modified to contain polyethylene glycol (PEG) to decrease surface charge and increase colloidal stability (Fig. 4) (Dubertret, 2002 ; Smith, 2006; You, 2007; Bagwe, 2003).

2.4 Biosensing based on biocompatible QDs

On the base of the synthetic methods of biocompatible QDs, water-soluble QDs can be covalently or electrostatically bound to a biological target, which have also acted as a new class of sensor. If the QDs encapsulated in amphiphilic polymers and PEG conjugated to antibodies, it would yield specificity for a variety of antigens. In addition, QDs cross-linked to other small molecule ligands, inhibitors, peptides, or aptamers can bind with many different cellular receptors and targets (Fig. 5) (Lidke, 2004; Xing, 2007). Gao and coworkers developed multifunctional nanoparticle probes based on semiconductor QDs for prostate

cancer targeting and imaging (Gao, 2004). The probes with passive and active tumor targeting behaviors were produced. This new class QDs probes contain an amphiphilic tri-block copolymer for in vivo protection, targeting-ligands for tumor antigen recognition and multiple PEG molecules for improved biocompatibility and circulation [Fig. 5(a)]. In the passive mode, antigenic tumors produce vascular endothelial growth factors, which can hyper-permeabilize the tumor-associated neovasculatures and cause the leakage of circulating macromolecules and small particles, leading to macromolecule or nanoparticle accumulation [Fig. 5(b)] (Gao, 2004; Duncan, 2003; Jain, 1999, 2001). While for active tumor targeting, antibody-conjugated QDs can track a prostate-specific membrane antigen (PSMA), which could be selected as an attractive target for imaging and therapeutic intervention of prostate cancer [Fig. 5(b)] (Gao, 2004; Schulke, 2003). This study opens new possibilities for ultrasensitive and simultaneous imaging of multiple biomarkers involved in cancer metastasis and invasion.

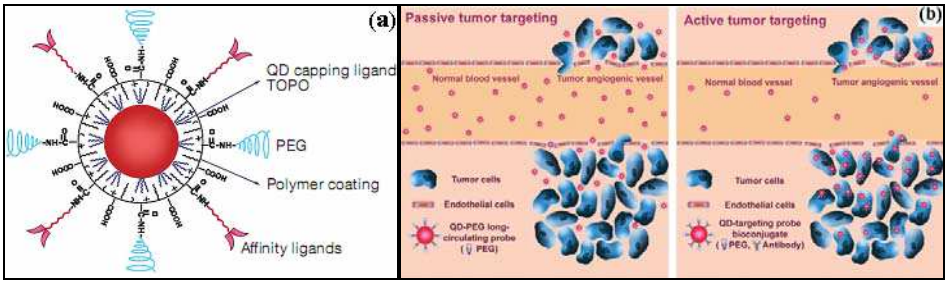

Fig. 5. Schematic illustration of bioconjugated QDs for in vivo cancer targeting and imaging. (a) Structure of a multifunctional QD probe; (b) Permeation and retention of QD probes via leaky tumor vasculatures (passive targeting) and high affinity binding of QD-antibody conjugates to tumor antigens (active targeting) (Gao, 2004).

Subsequently, Wu and coworkers demonstrated the use of 535QD-IgG and red 630QD-streptavidin to detect Her2 on the cell surface and nuclear antigens in the nucleus of SK-BR-3 cells. When the sample was observed under a fluorescence microscope, 630QD-labeled (red) nuclear antigens and 535QD-labeled (green) membrane-associated Her2 were visible simultaneously (Wu, 2003). This indicated that QDs conjugated to different secondary detection reagents can effectively detectect two cellular targets in the same cell. These results demonstrated the practicality of QDs in biological cellular real time and dynamic state imaging fields.

Fluorescence resonance energy transfer (FRET) is most commonly utilized in biosensors for detecting maltose (Medintz, 2003), aptamers (Hansen, 2006), 2,4,6-trinitrotoluene (Goldman, 2005), toxins (Goldman, 2004), and DNA (Zhang, 2005). Because of their high sensitivity, good reproducibility, and real-time monitoring capabilities, QDs are usually acted as fluorescence donors and make up of FRET with organic dyes. Medintz and coworkers designed a maltose sensor [Fig. 6(a)], in which an organic dye QSY-9 (fluorescence acceptor) was first conjugated to β-cyclodextrin (β-CD), then bonded to maltose binding protein (MBP), and at last β-CD-QSY-9/MBP complex was attached to the 560 QDs (fluorescence donors) surface through a peptide His-tag (Medintz, 2003). The optimized sensor contained 10 copies of β-CD-QSY9 bound to the QD complex, where 75% of the QD fluorescence was quenched by QSY-9. When free maltose was added, it would displace the β-CD-QSY9.

Moreover, the displacement of β-CD-QSY-9 with maltose could result in QD fluorescence increasing about 3-fold. This technique can be used to achieve the sensing of maltose. However, due to the uncertainty in the distance between the QDs and acceptors, some limitations in this sensor were arisen. In order to overcome the limitations, another maltose sensor was architected [Fig. 6(b)], in which 10 copies of Cy3 labeled MBP were first incorporated on the 530QDs surface, followed by binding of the Cy3.5 labeled β-CD, at last β-CD-Cy3.5/MBP-Cy3 complex was bound to QD through a peptide His-tag and Cy3.5 fluorescence emitted through a two-step FRET process. Sufficient fluorescence energy was initially transferred from the 530QD to MBP-Cy3, and the minimized emission energy of Cy3 was then transferred to β-CD-Cy3.5. When free maltose was added, the displacement of β-CD-Cy3.5 with maltose resulted in fluorescence increasing from Cy3 and concomitantly fluorescence decreasing from Cy3.5. The results demonstrate that the appropriately designed QD complexes with peptide immobilization tags can be used in determining small molecule concentrations in the 100 nM-10 μM range (Medintz, 2003)

Another biosensor based on combination of QDs and multi-walled carbon nanotubes (CNT) makes the detection of DNA and antigen more quickly and simply. Cui *et al* reported a highly selective, ultrasensitive, fluorescent detection method for DNA and antigen based on self-assembly of multi-walled carbon nanotubes (CNT) and CdSe QDs via oligonucleotide hybridization (Cui, 2008). This method could achieve the detection limit of 0.2 pM DNA molecules and 0.01 nM antigen molecules, and the novel detection system not only can be used for multicomponent detection and antigen-antibody immunoreaction, but also has great potential in photoelectrical biosensing application.

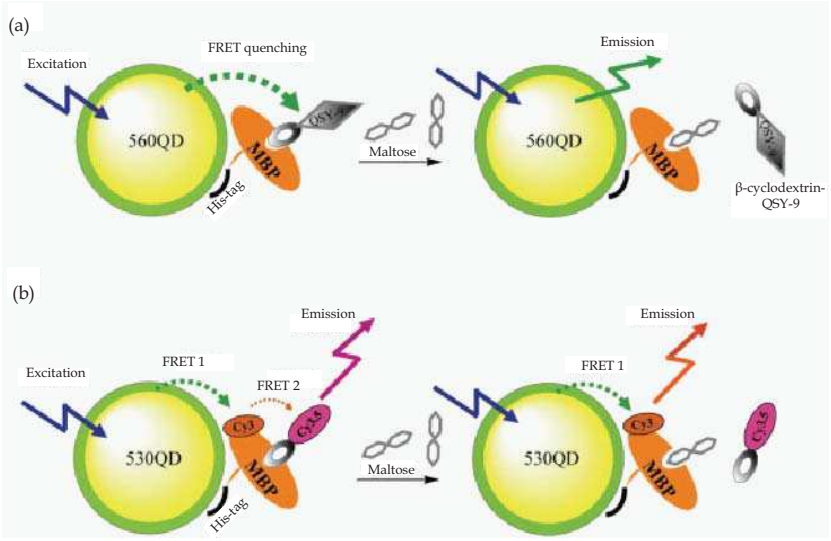

Fig. 6. QD based maltose nanosensor. (a) β-CD-QSY-9/MBP complex bound to QD through a peptide His-tag; (b) β-CD-Cy3.5/MBP-Cy3 complex bound to QD through a peptide His-tag (Zhou, 2007).

Recent advances in single-molecule detection, aptameric sensors with the surface functionalizing QDs hold exciting promise for many potential applications. Zhang *et al*

developed a single-QD-based aptameric sensor through (FRET) between 605QD and Cy5 and Iowa Black RQ (Zhang, 2009). This aptamertic sensor can recognize cocaine through both signal-off and signal-on modes, indicating the higher sensitivity and more extremely low sample consumption than that of the aptameric sensors established before. With the development of aptamers for small molecules, nucleic acids, metal ions, and proteins, this single-QD-based aptameric sensor might find wide application in forensic analysis, environmental monitoring, and clinic diagnostics (Zhang, 2009).

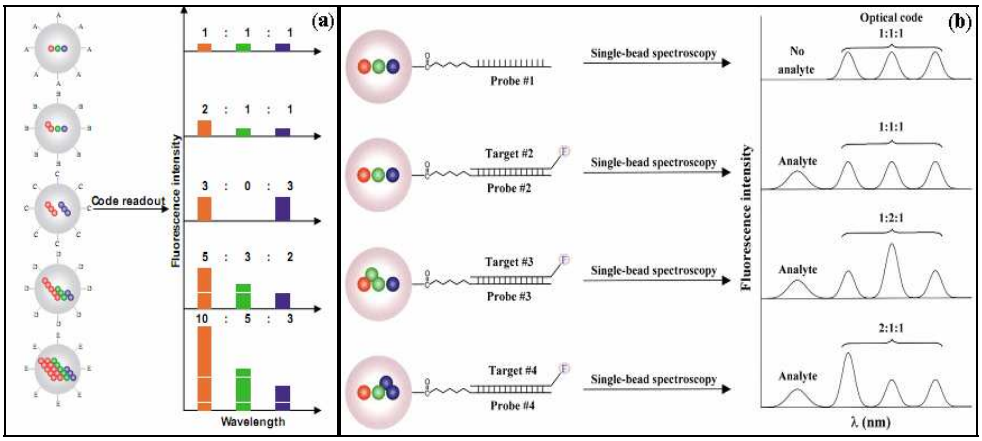

Fig. 7. Schematic illustrations of optical coding and DNA hybridization assays using QD-tagged beads (a) Optical coding based on wavelength and intensity multiplexing. Large spheres represent polymer microbeads, in which small multicolor QDs are embedded according to predetermined intensity ratios; (b) DNA hybridization assays using QD-tagged beads. Probe oligos were conjugated to the beads by crosslinking, and target DNA molecules were detected with a blue fluorescent dye such as Cascade Blue (Han, 2001).

Han and coworkers synthesized monodispersed CdSe/ZnS QDs with fluorescence emission at three primary colors (red, green and blue) (Han, 2001). Through embedding different-sized QDs into polymeric microbeads at precisely controlled intensity ratios [Fig. 7(a)], multicolor-tagged beads were prepared. Code readout is accomplished by measuring the fluorescence spectra of single beads. Their fluorescence emission wavelength can be continuously tuned by changing the particle size, and a single wavelength can be used for simultaneous excitation of different-sized QDs (Alivisatos, 1996; Han, 2001, Nirmal, 1999). On the other hand, molecular probes (A-E) may be attached to the bead surface for biological binding and recognition, such as DNA-DNA hybridization. In order to demonstrate the use of QD-tagged beads for DNA hybridization, oligonucleotide probes were conjugated to the beads by cross-linking. Target DNA molecules are directly labeled with a blue fluorescent dye such as Cascade Blue [Fig. 7(b)] (Han, 2001). Optical spectroscopy at the single-bead level yields both the coding and the target signals. Moreover, each color code corresponds to a specific DNA sequence. The coding signals can identify the DNA sequence, whereas the target signal can indicate the abundance of that sequence. A surprising finding is that the number of codes increases exponentially when multiple wavelengths and intensities are used simultaneously, for example, a

3-color/10-intensity scheme yields 999 codes, whereas a 6-color/10-intensity scheme has a theoretical coding capacity of about one million. In general, n intensity levels with m colors generate (n^m-1) unique codes (Han, 2001). If every code corresponds one type specific DNA sequence, it would be labeled every biomolecules with fluorescent code. This system made by multicolor-tagged QDs will completely change the ability of human identifying gene.

3. Rare-earth up-converting nanoparticles as fluorescent labels for biosensing application

3.1 Up-converting luminescence mechanism

Up-conversion (UC) refers to nonlinear optical processes characterized by the successive absorption of two or more pump photons via intermediate long-lived energy states followed by the emission of the output radiation at a shorter wavelength than the pump wavelength. UC processes are mainly divided into three broad classes: excited state absorption (ESA), energy transfer up-conversion (ETU), and photon avalanche (PA). All these processes involve the sequential absorption of two or more photons (Fig. 8).

In the case of ESA, the excitation takes the form of successive absorption of pump photons by a single ion. This is the basic process of up-conversion [Fig. 8(a)]. If the excitation energy is resonant with the transition from ground level G to excited metastable level E1, the phonon absorption occurs and populates E1 from G in a process known as ground state absorption (GSA). A second pump photon that promotes the ion from E1 to higher-lying state E2 results in UC emission, corresponding to the E2-G optical transition (Wang, 2009).

ETU is similar to ESA in that both processes utilize sequential absorption of two photons to populate the metastable level. The essential difference between ETU and ESA is that the excitation in ETU is realized through energy transfer between two neighboring ions. In an ETU process, each of two neighboring ions can absorb a pump phonon of the same energy, thereby populating the metastable level E1 [Fig. 8(b)]. A non-radiative energy transfer process promotes one of the ions to upper emitting state E2, while the other ion relaxes back to ground state G. The dopant concentration that determines the average distance between the neighboring dopant ions has a strong influence on the UC efficiency of an ETU process (Wang, 2009).

The phenomenon of PA was first discovered by Chivian and co-workers in Pr^{3+}-based infrared quantum counters (Chivian, 1979). PA-induced UC features an unusual pump mechanism that requires pump intensity above a certain threshold value. The PA process starts with population of level E1 by non-resonant weak GSA, followed by resonant ESA to populate upper visible-emitting level E2 [Fig. 8(c)]. After the metastable level population is established, the cross-relaxation energy transfer or ion pair relaxation occurs between the excited ion and a neighboring ground state ion, resulting in both ions occupying the intermediate level E1. The two ions readily populate level E2 to further initiate cross-relaxation and exponentially increase level E2 population by ESA, producing strong UC emission as an avalanche process (Wang, 2009).

The UC luminescent efficiency in these three processes varies considerably. ESA is the least efficient UC process. Efficient UC is possible in PA with metastable, intermediate levels that can act as a storage reservoir for pump energy. However, the PA process suffers from a number of drawbacks, including pump power dependence and slow response to excitation (up to several seconds) due to numerous looping cycles of ESA and cross-relaxation

processes. In contrast, ETU is instant and pump power independent, and thus has been widely used to offer highly efficient UC (Wang, 2009; Auzel, 2004).

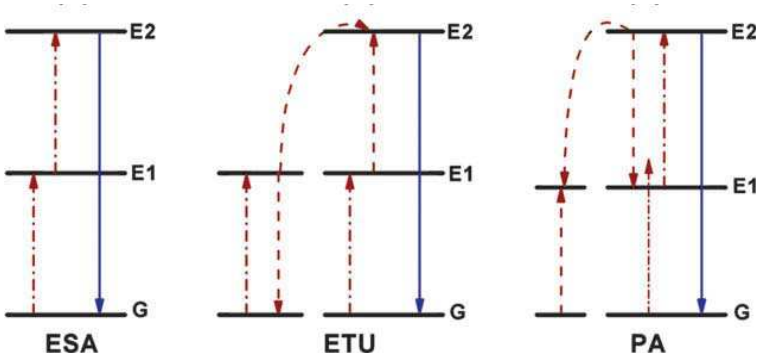

(a) (b) (c)

Fig. 8. Three energy transferring process diagrams of UC processes. (a) ESA; (b) ETU; (c) PA. The dashed/dotted, dashed, and full arrows represent photon excitation, energy transfer, and emission processes, respectively (Wang, 2009).

3.2 Synthesis of up-converting nanoparticles

For biological applications, UCNs should have a suitable size and surface for conjugation with biological molecules, and exhibit high intensity emission (Pires, 2006). Therefore, the synthesis of UCNs is particularly important. In general, the co-precipitation, thermal decomposition and hydro/solvo-thermal methods are most effective ways for synthesis of UCNs.

Co-precipitation is one of the most convenient techniques for synthesizing ultra-small UCNs with narrow size distribution. One of the earliest examples of this technique was demonstrated by van Veggel and co-workers, who made down-conversion LaF_3 nanocrystals doped with Ln^{3+} (Ln =Eu, Er, Nd, and Ho) (Stouwdam, 2002). The approach was expanded and refined by Chow *et al* (Yi, 2005), and UC LaF_3 nanocrystals with smaller particle size and narrower size distribution were obtained by using simple water soluble inorganic precursors. Besides, LaF_3, $NaYF_4$:Yb/Er(Tm), $LuPO_4$:Yb/Tm, and $YbPO_4$:Er nanocrystals were also synthesized via the co-precipitation approach (Heer, 2003, 2004; Yi, 2004; Zeng, 2005). The co-precipitation method is simple and quick, needing no expensive equipment and complex procedures, but requires post-heat treatment.

The thermal decomposition method is based on temporal separation of nucleation and crystal growth. It was firstly demonstrated for synthesis of highly monodispersed LaF_3 nanocrystals by Yan's group (Zhang, 2005). Later, this approach was extended as a common route to the synthesis of high quality UC $NaYF_4$ nanocrystals (Mai, 2006, Boyer, 2007). Zhao *et al* synthesized UC $NaYF_4$ nanorods, nanotubes, and flower-patterned nanodisks by an oleic acid-mediated hydrothermal method (Zhang, 2007). Recently, LaF_3:Yb/Er(Tm,Ho) nanoplates with multicolor UC luminescence were also successfully synthesized via a hybrid thermal decomposition/solvothermal method (Liu, 2007), which shows the superiorities in controlling the particle size and shape of the UCNs. However, this method needs specialized reaction vessels, expensive and air-sensitive precursors.

3.3 Optical properties of up-converting nanoparticles

Luminescent materials can absorb energy and subsequently emit the absorbed energy as radiation. According to the relative frequencies of the exciting and emitting radiations, radiant emission can be categorized into two classes of up-conversion and down-conversion. In the down-converting process, the emitting radiation obeys Stokes' law, in which the emitting radiation is of a lower energy and hence longer wavelength than the exciting light. However, for UCNs, the emitting radiation actually possesses a higher energy and smaller wavelength than the exciting wavelength, which is so-called anti-Stokes emission. As luminescent labeling materials, UCNs also show their superiority in several aspects comparing with conventional fluorescent dye or protein labels and QDs tags.

Firstly, UCNs are little analogous to QDs, even though QDs also hold a sharp emission bandwidth, long lifetime, tunable emission, high photostability and biocompatibility. The excitation and emission wavelength of UCNs are well separated from each other, which are ideal for multiplexing biological detection. Moreover, UCNs is generally made up of an inorganic host and lanthanide dopant ions embedded in the host lattice [Fig. 9(a)]. In the realization of UC processes, the crystal structure and optical property of host materials play important roles and require careful consideration. The luminescence emitted by UCNs is also dependent on the particle sizes, but it is different from quantum confinement effects as seen in QDs. The emission spectrum and color of the UCNs are associated with the host composition and particle surface properties (Lim, 2010; Mai, 2007). Generally, visible optical emissions under low pump power densities (ca. 10 W/cm^2) are only generated by using Er^{3+}, $Tm^{3+}$and Ho^{3+} as activators. In order to enhance up-converting efficiency, Yb^{3+} with a larger absorption cross-section in the NIR spectral region is frequently doped as a sensitizer in combination with the activators. In addition, UCNs can emit multicolor through the use of lanthanide-doped $NaYF_4$ nanoparticles with varied dopant ratios [Fig. 9 (d)].

Secondly, UCNs absorb NIR light and emit in the NIR or visible ranges, therefore, the penetration of NIR and the absence of autofluorescence background make the UCNs own unique ability of being imaged at a greater tissue depth. UC processes primarily rely on the ladder-like arrangement of energy levels of lanthanide dopant ions, and UC luminescence primarily originates from electron transitions between energy levels of localized dopant ions [Fig. 9(b)]. In case of the commonly used $NaYF_4$:Yb,Er nanoparticles, there are two emission peaks, one in the green region and the other in the red region [Fig. 9(c)] (Li, 2006). Recent studies show that lanthanide ions typically show a distinct set of sharp emission peaks, thus providing distinguishable spectroscopic fingerprints for accurate interpretation of the emission spectra in the event of overlapping emission spectra (Wang, 2009).

Thirdly, the UCNs are also resistant to photobleaching. A dried sample of PEI/$NaYF_4$ nanoparticles displayed no reduction in emission intensity when continually exposed to a 980 nm laser for over 7 h (Chatterjee, 2008). In addition, UCNs have lower cytotoxicity than QDs and exhibit almost no temporary and random loss of fluorescence (photo-blinking), as observed in semiconductor QDs.

3.4 Surface modification and functionalization of up-converting nanoparticles

For biological labeling applications, UCNs not only should exhibit high UC luminescence efficiency, but also need compatible with biomolecules. Most UCNs prepared by conventional strategies have no intrinsic aqueous solubility or lack functional organic moieties. Therefore, it is necessary that an additional surface treatment step should be required before bioconjugation.

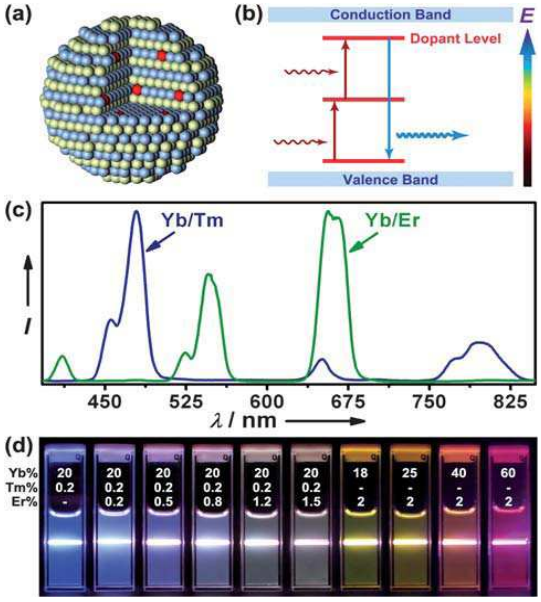

Fig. 9. (a) Structural diagram of UC nanoparticles; (b) Energy level diagram; (c) Emission spectra of cubic $NaYF_4$:Yb/Tm (20/0.2 mol%) and $NaYF_4$: Yb/Er (18/2 mol%) nanoparticles; (d) Fine tunable UC colors by adjusting the dopant ratios of lanthanide-doped $NaYF_4$ nanoparticles (Wang, 2008, 2010).

Ligand engineering, including ligand exchange, surface oxidation, ligand attraction, layer-by-layer assembly, and surface polymerization, is a common approach to generate a pendant functional group on the surface of UCNs (Fig. 10). Ligand exchange is normally realized by the reaction of UCNS with hydrophilic bifunctional molecules; while surface oxidation could be achieve by oxidizing the terminal group of native ligands to generate a pendant carboxylic functional group. Ligand attraction involves absorption of an additional amphiphilic polymer onto the nanoparticle surface through the hydrophobic van der Waals attraction between the original ligand and hydrocarbon chain of the polymer. Layer-by-layer assembly could be employed for electrostatic absorption of alternately charged polyions on the nanoparticle surface. Surface polymerization involves growing a dense cross-linked shell on the nanoparticle core by condensation of small monomers. Importance for these methods is the surface coverage with molecules consisting of additional functional groups that allow further reactions with biological entities (Cao, 2010; Boyer, 2010; Zhou, 2010; Kobayashi, 2009; Qian, 2008; Ehlert, 2008; Johnson, 2010). To some extent, the coating methods usually lead to highly stable colloidal particles in comparison with the ligand engineering method. Moreover, among various surface-coating methods, silica coating enjoys common usage by several groups, partly due to the well-established
surface chemistry of silica coating for facile bioconjugation. Distinctive feature of modified and functionalized up-converting nanoparticles is the retention of the native surface structures, thereby reducing the possibility of creating surface defects that quench the UC luminescence. However, surface modification sometimes adversely affects photophysical properties of up-converting nanoparticles.

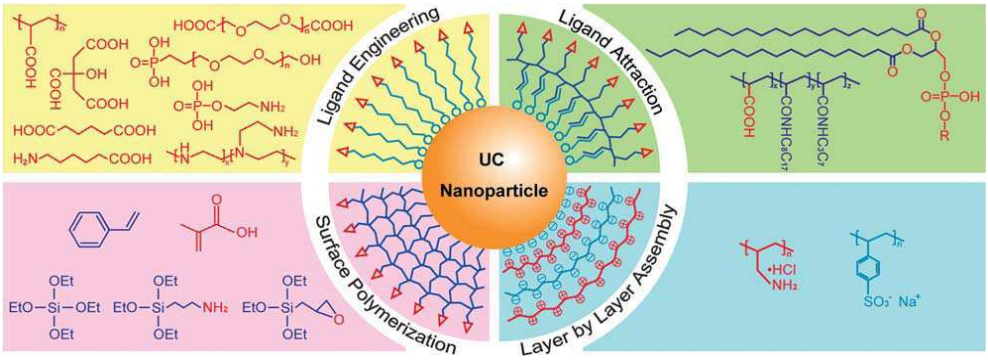

Fig. 10. Typical strategies for solubilization and functionalization of UCNs (Wang, 2010).

3.5 Application of up-converting nanoparticles for biological sensing

Application of UCNs for biological sensing can be roughly divided into two classes: one is directly observed luminescence from the UCNs, and the other is based on FRET. UCNs have been used as luminescent reporters in a variety of assays, including immune-assay, bio-affinity assay, and DNA hybridization assay as alternatives to conventional labeling agents (Zijlmans, 1999; Hampl, 2001; Corstjens, 2008; Li, 2008; Huang, 2009). A example was demonstrated by submicron-sized Y_2O_2S particles doped with Yb^{3+} and Er^{3+} ions for detection of human chorionic gonadotropin with a limit of 10 pg in a lateral flow (LF) immune-chromatographic assay format (Hampl, 2001). Another intriguing example has been demonstrated by Niedbala's group (Niedbala, 2001), in which an LF-based strip assay for the simultaneous detection of amphetamine, methamphetamine, phencyclidine, and opiates in saliva was developed by using multicolor UC particles. The architecture of the lateral flow strip is designed to accommodate up to 12 distinct test lines, in which green emitting particles were coupled to antibodies for phencyclidine and amphetamine, and blue emitting particles were coupled to antibodies for methamphetamine and morphine. In addition, each strip also contains two control lines. By analyzing the test strip for each colored phosphor, the drug molecules (amphetamine, methamphetamine, phencyclidine, and opiates) were successfully detected. The whole process was very short less than 10 min and with high sensitivity.

UCNs have also been coupled with metallic nanoparticles or organic fluorophores for FRET based biosensing. Wang *et al* developed a highly sensitive biosensor for detection of avidin by using biotinylated $NaYF_4$:Yb/Er nanoparticles as energy donors and biotinylated Au nanoparticles as energy acceptors. The 7 nm Au nanoparticles show a broad and strong absorption centered at 520 nm, which matches well with the 540 nm emission of $NaYF_4$:Yb/Er nanoparticles. Biotinylated $NaYF_4$:Yb/Er and Au nanoparticles with molecular probes can specifically interact between avidin and biotin. When the target is absent, the donor and acceptor are well separated and no FRET process is expected. In the presence of the target, the donor and acceptor will be linked in close proximity and FRET becomes significant, resulting in a decrease in emission intensity of the donor. In addition, due to UCNs with ability of reducing background autofluorescence, UCNs have also been used as luminescent reporters in genomic applications (Corstjens, 2001). As a derivative of FRET, luminescence resonance energy transfer (LRET) was firstly introduced as by Selvin

(Selvin, 1994, 2002). LRET mainly relies on the same dipole-dipole mechanism as conventional FRET, but it has its own advantage, which offers a large energy transfer distance range (>10 nm) and high reliability. Particularly, the long-lived luminescent lanthanide donors allow facile and accurate lifetime measurements to monitor biological events that are inaccessible with conventional fluorescent dyes.

UC particles have also been used in genomic biosensor. Due to the elimination of unwanted autofluorescence, UC particles can facilitate the detection and handling of target molecules by shortening the polymerase chain reaction (PCR) amplification process. In a parallel development, Wang and Li demonstrated a sandwich-hybridization assay for the ultra-sensitive detection of DNA using sub-50 nm $NaYF_4$:Yb/Er nanoparticles (Wang, 2006). Among this assay system, UCNs are modified with probe DNA strands, while magnetic nanoparticles are used and modified capture DNA strands. Upon incubation with target DNA strands, the UC and magnetic nanoparticles form binary nanoparticle aggregates. By virtue of magnetic nanoparticles, the aggregates can be easily purified and examined via UC luminescence assays (Fig. 11). Moreover the lowest detection limit of this method is ca. 10 nM and without PCR amplification.

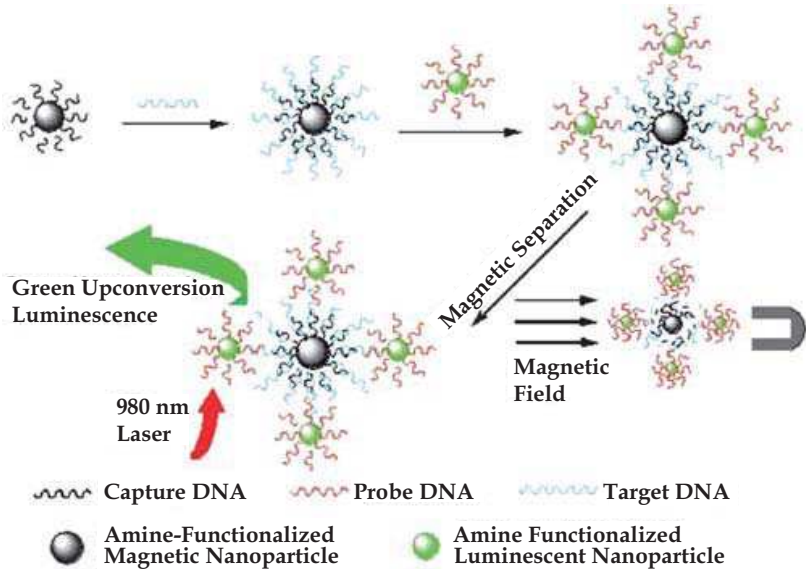

Fig. 11. Schematic illustration of the UC nanoparticle and magnetic nanoparticles-based DNA detection (Wang, 2006).

4. Comparative assessment of semiconductor QDs and rare-earth up-converting nanoparticles for biosensing application

Semiconductor QDs possess high photostability, tunable emission spectra, high quantum yields, narrow emission bandwidths, superior signal brightness, long fluorescence lifetimes, and rich surface coupling capability, so they have been widely used in a variety of biosensors (Alivisatos, 2005). QDs are down-converting materials, which emit visible

fluorescence when excited by ultraviolet (UV) light or short wavelength visible light. However, when using UV light for monitoring living processes in cells and tissues, there have some potential drawbacks. In particular, if using UV light long-term irradiates living cells, it may cause DNA damage, cell death and reduce the signal-to-background ratio. Furthermore, in vivo fluorescence imaging is limited by the short penetration depth of the excitation light. In the most case, QDs have resistance to photobleaching, but sometimes they do exhibit temporary and random loss of fluorescence (photo-blinking). Currently, there are a class of NIR fluorophores such as NIR fluorescent dyes and the developed NIR quantum dots (Zhang, 2007). Though they own the abilities of deep tissue penetration and low autofluorescence as compared to visible fluorophores, they also have some disadvantages to signal detection. NIR detectors and filters are needed and the excitation and emission wavelengths are too close to each other. Furthermore, NIR dyes experienced photo-bleach and NIR QDs are cytotoxic. These factors greatly limit their application in biosensor.

Compared with QDs, UCNs absorb NIR light and emit in the NIR or visible ranges, and the excitation and emission wavelength are well separated from each other. Meanwhile, since different colored emission peaks have little overlap, sharp emission peaks, it is ideal for multiplexing bio-detection. More importantly, NIR radiation is less harmful to cells and minimizes autofluorescence from biological tissues, thereby increasing the signal-to-noise ratio significantly. UCNs exhibit almost no temporary and random loss of fluorescence (photo-blinking) as observed in QDs, which is beneficial for accurate tracking of individual UCNs (Frangioni, 2003). Of course, UCNs also own themselves shortcoming, for example, the determination of the quantum yield of UCNs becomes difficult because the standards that show up-conversion property are not available. Boyer *et al* have determined and reported the quantum yield of $NaYF_4$ UCNs with various sizes, and their quantum yields vary from 0.005% to 0.3% (Boyer, 2010). This is comparatively lower than the quantum yield of QDs, which quantum yields could attain 5-85% (Wang, 2003; Shavel, 2006). Therefore, these factors also limit, to some degree, the application of UCNs in biosensing fields.

5. Concluding remarks and perspective

This paper reviews the latest research advances in utilization of QDs and UCNs conjugates in biosensing fields based on their unique optical properties. The advantages and limitation of QDs and UCNs for biosensing applications are comparatively summarized. QDs conjugates were widely attempted in uses for imaging, targeting drug, and biosensing fields. However, the photo-blinking phenomenon, high background autofluorescence from biological tissues and toxicity to living system of QDs largely affect their potentials in biosensing application. To conquer these challenges, great efforts need to be made in control synthesis, surface modification and functionalization, luminescence modulation, and bioconjugation technology of semiconductor QDs to further improve their chemical photostability, spectra availability, surface chemistry, understand their pharmacokinetics, metabolism, degradation and safety in living system, and reduce the and toxicity. Moreover, the design and synthesis of high quality QDs with efficient NIR emission and non-toxic element composition is also desired for raising the availability of QDs in biological application. The last but not the least, with the development of QDs in biosensing application, new instrumentation and platform by integration of QDs with multifunctional

nanosystem that can target, sense, image and treat diseases are also necessary to push basic research moving to clinic trial.

Partially different from semiconductor QDs, UCNs show features of chemical stability, resistance to photobleaching, large anti-Stokes shift, sharp emission peaks, and non-toxicity. Moreover, due to their unique visible emission excited by NIR light, UCNs show advantages of the deep penetration in tissue and the absence of background autofluorescence in biosensing application. However, there are still challenges for UCNs to become ideal biological labels for practical biosensing application. One of the biggest challenges that hurdles UCNs to practically used in biosensor is that the quantum yield of the UCNs is quite low, which results in the low fluorescence signals. In a relatively complicated biosensing process, the fluorescence signal may be hard to capture with normal instrumentation when using UCNs as fluorescent labels. In addition, the surface modification and functionalization of UCNs for improving their quantum yield need to be further consummated. The lack of common recognized approach and standard for determining the quantum yield of UCNs might be another challenge. The controlled synthesis and surface modification of UCNs that exhibit high colloidal stability and tailorable optical properties is always desired. Substantial efforts are also needed to focus on development of strategies for patterning UCNs on various substrates, allowing for multiplexed high-sensitivity detection in biosensor.

6. Acknowledgements

We gratefully acknowledge the financial supports from National High Technology Research and Development Program (863 program, 2010AA03A407), National Natural Science Foundation of China (20961005), Department of Science and Technology of Inner Mongolia (Public Security Foundation 208096), Inner Mongolia University Funds (10013-121008).

7. References

Alivisatos A. P. (2004). The use of nanocrystals in biological detection. *Nat. Biotechnol.,* Vol. 22, pp. 47-52.

Alivisatos A. P. (1996). Perspectives on the physical chemistry of semiconductor nanocrystals. *J. Phys. Chem.*, Vol. 100, pp. 13226-13239.

Alivisatos A. P. (1996). Semiconductor clusters, nanocrystals, and quantum dots. Science, Vol. 271, pp. 933–937.

Alivisatos A. P. Gu W. Larabell C. (2005). Quantum dots as cellular probes. *Annu. Rev. Biomed. Eng*., Vol. 7, pp. 55–76.

Auzel F. (2004). Upconversion and anti-Stokes processes with f and d ions in solids. *Chem. Rev*., Vol. 104, pp. 139-174.

Bagwe R. P. Zhao X. J. Tan W. H. (2003). Bioconjugated luminescent nanoparticles for biological applications. *J. Dispers. Sci. Technol.*, Vol. 24, pp. 453–464.

Blasse G. B. Grabmaier C. (1994). *Luminescent Materials*, Springer, Berlin

Boyer J. C. Cuccia L. A. Capobianco J. A. (2007). Synthesis of colloidal upconverting $NaYF_4$: Er^{3+}/Yb^{3+} and Tm^{3+}/Yb^{3+} monodisperse nanocrystals. *Nano Lett*., Vol. 7, pp. 847-852.

Boyer J. C. Manseau M. P. Murray J. I. van Veggel F. C. J. M. (2010). Surface modification of upconverting NaYF4 nanoparticles with PEG−phosphate ligands for NIR (800 nm) biolabeling within the biological window. *Langmuir*, Vol. 26, pp. 1157–1164.

Boyer J. C. van Veggel F. C. J. M. (2010). Absolute quantum yield measurements of colloidal $NaYF_4$:Er^{3+},Yb^{3+} upconverting nanoparticles. *Nanoscale,* Vol. 2, pp. 1417–1419.

Bruchez Jr M. Moronne M. Gin P. Weiss S. Alivisatos A. P. (1998). Semiconductor Nanocrystals as Fluorescent Biological Labels. *Science*, Vol. 281, pp. 2013-2016.

Brus L. E. (1984). Electron-electron and electron-hole interactions in small metallic crystallites: The size-dependence of the lowest optically excited electronic states. *J. Chem. Phys.*, Vol. 80, pp. 4403–4409.

Cao T. Y. Yang T. S. Cao Y. Yang Y. Hu H. Li F. (2010). Water-soluble NaYF4:Yb/Er upconversion nanophosphors: Synthesis, characteristics and application in bioimaging. *Inorg. Chem. Commun.*, Vol. 13, pp. 392–394.

Chan W. C. W. Nie S. (1998). Quantum Dot Bioconjugates for Ultrasensitive Nonisotopic Detection. *Science,* Vol. 281, pp. 2016-2018.

Chatterjee D. K. Rufaihah A. J. Zhang Y. (2008.) Upconversion fluorescence imaging of cells and small animals using lanthanide doped nanocrystals. *Biomaterials*, Vol. 29, pp. 937–943.

Chivian J. S. Case W. E. Eden D. D. (1979). *Appl. Phys. Lett.*, Vol. 35, pp. 35124.

Corstjens P. van Lieshout L. Zuiderwijk M. Kornelis D. Tanke H. J. Deelder A. M. van Dam. C. J. (2008). Up-converting phosphor technology-based lateral flow assay for detection of schistosoma crculating anodic antigen in serum. *J. Clin.Microbiol.*, Vol. 46, pp. 171–176.

Corstjens P. Zuiderwijk M. Brink A. Li S. Feindt H. Niedbala R. S. Tanke H. (2001). Use of up-converting phosphor rporters in lateral-flow assays to detect specific nucleic acid sequences: A rapid, sensitive DNA test to identify human papillomavirus type 16 infection. *Clin. Chem.*, Vol. 47, pp. 1885–1893.

Cui D. X. Pan B. F. Zhang H. Gao F. Wu R. Wang J. He R. Asahi T. (2008). Self-Assembly of Quantum Dots and Carbon Nanotubes for Ultrasensitive DNA and Antigen Detection. *Anal. Chem.*, Vol. 80, pp. 7996–8001.

Derfus A. M. Chan W. C. W. Bhatia S. N. (2004). Probing the cytotoxicity of semiconductor quantum dots. *Nano Lett.*, Vol. 4, pp. 11–18.

Dubertret B. Skourides P. Norris D. J. Noireaux V. Brivanlou A. H. Libchaber A. (2002). In vivo imaging of quantum dots encapsulated in phospholipid micelles *Science*, Vol. 298, pp. 1759–1762.

Duncan R. (2006), Polymer conjugates as anticancer nanomedicines. *Nat. Rev. Cancer*, Vol. 6, pp. 688–701.

Duncan R. (2003). The dawning era of polymer therapeutics. Nat. Rev. Drug Discov., Vol. 2, pp. 347–360.

Ehlert O. Thomann R. Darbandi M. Nann. T. (2008). A four-color colloidal multiplexing nanoparticle system. *ACS Nano*, Vol. 2, pp. 120–124.

Feldmann C. Goesmann H. (2010). Nanoparticulate functional materials. *Angew. Chem. Int. Ed.*, Vol. 49, pp. 1362-95.

Frangioni J. V. (2003). In vivo near-infrared fluorescence imaging. *Curr. Opin. Chem. Biol*. Vol. 7, pp. 626–634.

Gaponenko S. V. (1998). *Optical Properties of Semiconductor Nanocrystals.* Cambridge University Press, New York

Gao X. H. Cui Y. Y. Levenson R. M. Chung W. K. L. Nie S. (2004). In vivo cancer targeting and imaging with semiconductor quantum dots. *Nat. Biotechnol*., Vol. 22, pp. 969-976.

Gerion D. Pinaud F. Williams S. C. Parak W. J. Zanchet D. Weiss S. Alivisatos A. P. (2001). Synthesis and properties of biocompatible water-soluble silica-coated CdSe/ZnS semiconductor quantum dots, *J. Phys. Chem. B,* Vol. 105, pp. 8861–8871.

Goldman E. R. Clapp A. R. Anderson G. P. Goldman E. R. Clapp A. R. Anderson G. P. Uyeda H. T. Mauro J. M. Medintz I. L. Mattoussi H. (2004). Multiplexed toxin analysis using four colors of quantum dot fluororeagents. *Anal. Chem.,* Vol. 76, pp. 684–688.

Goldman E. R. Medintz I. L. Whitley J. L. Hayhurst A. Clapp A. R. Uyeda H. T. Deschamps J. R. Lassman M. E. Mattoussi H. (2005). A hybrid quantum dot−antibody rragment fluorescence resonance energy transfer-based TNT sensor. *J. Am. Chem. Soc*., Vol. 127, pp. 6744–6751.

Goronkim H. et al. (1999). *In Nanostructure Science and Technology*, a worldwide study. Eds. By Siegiel R. W., Hu E. and Rocco M. C., NSTC

Hampl J. Hall M. Mufti N. A. Yao Y. M. MacQueen D. B. Wright W. H. Cooper D. E. (2001). Upconverting phosphor reporters in immunochromatographic assays. *Anal. Biochem*., Vol. 288, pp. 176–187.

Han M. Y. Gao X. H. Su J. Z. Nie S. (2001). Quantum-dot-tagged microbeads for multiplexed optical coding of biomolecules. *Nat. Biotechnol*., Vol. 19, pp. 631-635.

Hansen J. A. Wang J. Kawde A. N. Xiang Y. Gothelf K. V. Collins G. (2006). Quantum-dot/aptamer-based ultrasensitive multi-analyte electrochemical biosensor. *J. Am. Chem. Soc*., Vol. 128, pp. 2228–2229.

Heer S. Kömpe K. Güdel H. U. Haase M. (2004). Highly efficient multicolour upconversion emission in transparent colloids of lanthanide-doped $NaYF_4$ nanocrystals. *Adv. Mater*., Vol. 16, pp. 2102-2105.

Heer S. Lehmann O. Haase M. Güdel H. U. (2003), Blue, green, and red upconversion emission from lanthanide-doped $LuPO_4$ and $YbPO_4$ nanocrystals in a transparent colloidal slution. *Angew. Chem. Int. Ed*., Vol. 42, pp. 3179-3182.

Hermanson G. T. (1996). *Bioconjugate Techniques.* Academic Press, New York

Hood J. D. Bednarski M. Frausto R. Guccione S. Reisfeld R. A. Xiang R. Cheresh D. A. (2002). Tumor regression by targeted gene delivery to the neovasculature, *Science*, Vol. 296, pp. 2404–2407.

Huang L. H. Zhou L. Zhang Y. B. Xie C. K. Qu J. F. Zeng A. J. Huang H. J. Yang R. F. Wang X. Z. (2009). Simple optical rader for upconverting phosphor particles captured on lateral flow strip. *J. IEEE Sens*., Vol. 9, pp. 1185–1191.

Jain. R. K. (2001). Delivery of molecular medicine to solid tumors: lessons from in vivo imaging of gene expression and function. *J. Control. Release*, Vol. 74, pp. 7–25.

Jain R. K. (1999). Transport of molecules, particles, and cells in solid tumors. *Annu. Rev.Biomed. Eng.*, Vol. 1, pp. 241–263.

Jaiswal J. K. Simon S. M. (2004). Potentials and pitfalls of fluorescent quantum dots for biological imaging. *Trends. Cell Biol.*, Vol. 14, pp. 497–504.

Johnson N. J. J. Sangeetha N. M. Boyer J. C. van Veggel F. C. J. M. (2010), Facile ligand-exchange with polyvinylpyrrolidone and subsequent silica coating of hydrophobic upconverting β-$NaYF^4$:Yb^{3+}/Er^{3+} nanoparticles. *Nanoscale*, Vol. 2, pp. 771–777.

Katz E. Willner I. (2004). Integrated nanoparticle-biomolecule hybrid systems: Synthesis, properties and applications. *Angew. Chem. Int. Ed.,* Vol. 43, pp. 6042-6108.

Kim J. H. Morikis D. Ozkan M. (2004), Adaptation of inroganic quantum dots for stable molecular beacons. *Sens Actuators B*, Vol. 102, pp. 315–319.

Kobayashi H. Kosaka N. Ogawa M. Morgan N. Y. Smith P. D. Murray C. B. Ye X. Collins J. Kumar G. A. Bell H. Choyke P. L. (2009). *In vivo* multiple color lymphatic imaging using upconverting nanocrystals. *J. Mater. Chem.*, Vol. 19, pp. 6481–6484.

Li J. J. Ouellette A. L. Giovangrandi L. Coope D. E. Ricco A J. Kovacs G. T. A. (2008). Optical scanner for immunoassays with up-converting phosphorscent labels. *IEEE Trans. Biomed. Eng.*, Vol. 55, pp. 1560–1571.

Li Z. Q. Zhang Y. (2006). Monodisperse silica-coated polyvinylpyrrolidone/NaYF4 nanocrystals with multicolor upconversion fluorescence emission. *Angew. Chem. Int. Ed.*, Vol. 45, pp. 7732 –7735.

Lidke D. S. Nagy P. Heintzmann R. Arndt-Jovin D. J. Post J. N. Grecco H. E. Jares-Erijman E. A. Jovin T. M. (2004). Quantum dot ligands provide new insights into erbB/HER receptor-mediated signal transduction. *Nat. Biotechnol.*, Vol. 22, pp. 198–203.

Lim S. F. Ryu W. S. Austin R. H. (2010). Particle size dependence of the dynamic photophysical properties of NaYF4:Yb, Er nanocrystals. *Opt. Express*, Vol. 18, pp. 2309-2316.

Liu C. Chen D. (2007). Controlled synthesis of hexagon shaped lanthanide-doped LaF_3 nanoplates with multicolor upconversion fluorescence. *J. Mater. Chem.*, Vol. 17, pp. 3875-3880.

Mai H. X. Zhang Y. W. Si R. Yan Z. G. Sun L. D. You L. P. Yan C. H. (2006). High-quality sodium rare-earth fluoride nanocrystals: controlled synthesis and optical properties. *J. Am. Chem. Soc.,* Vol. 128, pp. 6426-6436.

Mai H. X. Zhang Y. W. Sun L. D. Yan C. H. (2007). Highly efficient multicolor up-conversion emissions and their mechanisms of monodisperse NaYF4:Yb,Er core and core/shell-structured nanocrystals. *J. Phys. Chem. C,* Vol. 111, pp. 13721-13729.

Mansur H. S. (2010). Quantum dots and nanocomposites. *Wiley Interdisciolinary Reviews: Nanomedicine and Nanobiotechnology*, Vol. 2, pp. 113-129.

Medintz I. L. Clapp A. R. Mattoussi H. Goldman E. R. Fisher B. Mauro J. M. (2003). Self-assembled nanoscale biosensors based on quantum dot FRET donors. *Nat. Mater.*, Vol. 2, pp. 2, 630–638.

Murray C. B. Norris D. J. Bawendi M. G. (1993). Synthesis and characterization of nearly monodisperse CdE (E = sulfur, selenium, tellurium) semiconductor nanocrystallites. *J. Am. Chem. Soc.*, Vol. 115, pp. 8706–8715.

Murphy C. J. Coffer J. L. (2002). Quantum dots: A primer. *Appl. Spectrosc.*, Vol. 56, pp. 16A-27A.

Niedbala R. S. Feindt H. Kardos K. Vail T. Burton J. Bielska B. Li S. Milunic D. Bourdelle P. Vallejo R. (2001). Detection of analytes by imunoassay using up-converting phosphor technology. *Anal. Biochem.*, Vol. 293, pp. 22–30.

Nirmal M. Brus L. E. (1999). Luminescence Photophysics in Semiconductor Nanocrystals. *Acc. Chem. Res.*, Vol. 32, pp. 407–414.

Pires M. A. Heer S. Gudel H. U. Serra O.A. (2006). Er, Yb doped yttrium based nanosized phosphors: Particle size, "host lattice" and doping ion concentration effects on upconversion efficiency. *J. Fluoresc.*, Vol. 16, pp. 461- 468.

Qian H. S. Li Z. Q. Zhang Y. (2008). Multicolor polystyrene nanospheres tagged with up-conversion fluorescent nanocrystals. *Nanotechnology*, Vol. 19, pp. 255601.

Rosi N. L. Mirkin C. A. (2005). Nanostructures in biodiagnostics. *Chem. Rev.*, Vol. 105, pp. 1547-1562.

Selvin P. R. (2002). Principles and biophysical application of lanthanide-based probes. *Annu. Rev. Biophys. Biomol. Struct.,* Vol. 31, pp. 275-302.

Selvin P. R. Rana T. M. Hearst J. E. (1994). Luminescence resonance energy transfer. *J. Am. Chem. Soc.,* Vol. 116, pp. 6029–6030.

Shavel A. Gaponik N. Eychmüller A. (2006). Factors governing the 1uality of aqueous CdTe nanocrystals:Calculations and experiment. *J. Phys. Chem. B*, Vol. 110, pp. 19280–19284.

Smith A. M. Duan H.W. Mohs A. M. Nie S. (2008). Bioconjugated quantum dots for in vivo molecular and cellular imaging. *Adv. Drug Delivery Rev.*, Vol. 60, pp. 1226-1240.

Smith A. M. Duan H.W. Rhyner M. N. Ruan G. Nie S. (2006). A systematic examination of surface coatings on the optical and chemical properties of semiconductor quantum dots. *Phys. Chem. Chem. Phys.,* Vol. 8, pp. 3895–3903.

Stouwdam J. W. van Veggel F. C. J. M. (2002). Near-infrared emission of redispersible Er^{3+}, Nd^{3+}, and Ho^{3+} doped LaF_3 nanoparticles. *Nano Lett.*, Vol. 2, pp. 733-737.

Varlamova O. A. Donovan D. P. Ma D. Gardner J. P. Morrissey D. M. Arrigale R. R. Zhan C. Chodera A. J. Surowitz K. G. Maddon P. J. Heston W. D. W. Olson W. C. (2003). The homodimer of prostate-specific membrane antigen is a functional target for cancer therapy. *Proc. Natl. Acad. Sci.,* Vol. 100, pp. 12590–12595.

Wang F. Banerjee D. Liu Y. S. Chen X. Y. Liu X. G. (2010). Upconversion nanoparticles in biological labeling, imaging, and therapy. *Analyst*, Vol. 135, pp. 1839–1854.

Wang F. Liu X. G. (2009). Recent advances in the chemistry of lanthanide-doped upconversion nanocrystals. *Chem. Soc. Rev.*, Vol. 38, pp. 976-989.

Wang F. Liu X. G. (2008). Upconversion multicolor fine-tuning: Visible to near-infrared emission from lanthanide-doped $NaYF_4$ nanoparticles. *J. Am. Chem. Soc.*, Vol. 130, pp. 5642–5643.

Wang L. Y. Li Y. D. (2006). Green upconversion nanocrystals for DNA detection. *Chem. Commun.*, Vol. 24, pp. 2557–2559.

Wang L. Yan R. Huo Z. Wang L.Zeng J. Bao J. Wang X. Peng Q. Yadong Li. (2005). Fluorescence resonant energy transfer biosensor based on upconversion-luminescent nanoparticles. *Angew. Chem. Int. Ed*., Vol. 44, pp. 6054-6057.

Wang X. Qu L. Zhang J. Peng X. Xiao M. (2003). Surface-related emission in highly luminescent CdSe quantum dots. *Nano Lett.*, Vol. 3, pp. 1103–1106.

Weaver J. Zakeri R. Aouadi S. Kohli. P. (2009) Synthesis and characterization of quantum dot–polymer composites *J. Mater. Chem*., Vol. 19, pp. 3198-3206.

Weller H. (1993). Colloidal semiconductor Q-particles: chemistry in the transition region between solid states and molecules. *Angew. Chem. Int. Ed.,* Vol. 32, pp. 41-53.

Wu X. Y. Liu H. J. Liu J. Q. Wu, X. Y. Liu H. J. Liu J. Q. Haley K. N. Treadway J. A. Larson J. P. Ge, N. F. Peale F. Bruchez M. P. (2003). Immunofluorescent labeling of cancer marker Her2 and other cellular targets with semiconductor quantum dots. *Nat. Biotechnol*., Vol. 21, pp. 41–46.

Xing Y. Chaudry Q. Shen C. Kong K. Y. Zhau, H. E. W. Chung L. Petros. J. A. O'Regan R. M. Yezhelyev M .V. Simons J. W. Wang M. D. Nie S. (2007). Bioconjugated quantum dots for multiplexed and quantitative immunohistochemistry. *Nat. Protoc.*, Vol. 2, pp. 1152–1165.

Yen W. M. Weber M. J. (2004). *Inorganic phosphors: compositions, preparation and optical properties*. CRC Press, Florida

Yi G. Chow G. (2005). Colloidal LaF_3:Yb,Er, LaF_3:Yb,Ho and LaF_3:Yb,Tm nanocrystals with multicolor upconversion fluorescence. *J. Mater. Chem*., Vol. 15, pp. 4460-4464.

Yi G. Lu H. Zhao S. Ge Y. Yang W. Chen D. Guo L. (2004). Synthesis, characterization, and biological application of size-controlled nanocrystalline NaYF4:Yb,Er infrared-to-visible up-conversion phosphors. *Nano Lett*., Vol. 4, pp. 2191-2196.

You C. C. Chompoosor A. Rotello V. M. (2007). The biomacromolecule-nanoparticle interface, *Nano Today*, Vol. 2, pp. 34–43.

Zeng J. Su J. Li Z. Yan R. X. Li Y. D. (2005). Synthesis and upconversion luminescence of hexagonal-phase $NaYF_4$:Yb, Er^{3+} phosphors of controlled size and morphology. *Adv. Mater.*, Vol. 17, pp. 2119-2123.

Zhang C. Y. Johnson L. W. (2009). Single Quantum-Dot-Based Aptameric Nanosensor for Cocaine. Anal. *Chem*., Vol. 81, pp. 3051–3055.

Zhang C. Y. Yeh H. C. Kuroki M. T. Wang T. H. (2005). Single-quantum-dot-based DNA nanosensor. *Nat. Mater*., Vol. 4, pp. 826–831.

Zhang F. Wan Y. Yu T. Zhang F. Shi Y. Xie S. Li Y. Xu L. Tu B. Zhao D. (2007). Uniform nanostructured arrays of sodium rare-earth fuorides for highly efficient multicolor upconversion luminescence. *Angew. Chem. Int. Ed*., Vol. 46, pp. 7976-7979.

Zhang J. Su J. F. Liu L. Huang Y. Mason R. P. (2007). Evaluation of red CdTe and NIR CdHgTe QDs by fluorescent imaging. *J. Nanosci. Nanotechnol.,* Vol. 8, pp. 1155-1159.

Zhang J. Z. (1997). Ultrafast studies of electron dynamics in semiconductor and metal colloidal nano-particles: effects of size and surface. *Acc. Chem. Res*., Vol. 30, pp. 423-429.

Zhang Y. W. Sun X. Si R. You L. P. Yan C. H. (2005). Single-crystalline and monodisperse LaF_3 triangular nanoplates from a single-source precursor. *J. Am. Chem. Soc.*, Vol. 127, pp. 3260-3261.

Zhou J. Sun Y. Du X. Xiong L. Hu H. Li F. (2010). Dual-modality in vivo imaging using rare-earth nanocrystals with near-infrared to near-infrared (NIR-to-NIR) upconversion luminescence and magnetic resonance properties. *Biomaterials,* Vol. 31, pp. 3287–3295.

Zhou M. Ghosh I.(2007). Quantum dots and peptides: A bright future together. *Peptide Science,* Vol. 88, pp. 325-339.

Zijlmans H. Bonnet J. Burton J. Burton J. Kardos K. Vail T. Niedbala R. S. Tanke H. J. (1999). Detection of cell and tissue srface antigens using up-converting phosphors: A new rporter technology. *Anal. Biochem*., Vol. 267, pp. 30–36.

New Perspectives in Biosensors Technology and Applications

Edited by Prof. Pier Andrea Serra

ISBN 978-953-307-448-1
Hard cover, 448 pages
Publisher InTech
Published online 27, July, 2011
Published in print edition July, 2011

A biosensor is a detecting device that combines a transducer with a biologically sensitive and selective component. Biosensors can measure compounds present in the environment, chemical processes, food and human body at low cost if compared with traditional analytical techniques. This book covers a wide range of aspects and issues related to biosensor technology, bringing together researchers from 12 different countries. The book consists of 20 chapters written by 69 authors and divided in three sections: Biosensors Technology and Materials, Biosensors for Health and Biosensors for Environment and Biosecurity.

INTECH
open science | open minds

InTech Europe
University Campus STeP Ri
Slavka Krautzeka 83/A
51000 Rijeka, Croatia
Phone: +385 (51) 770 447
Fax: +385 (51) 686 166
www.intechopen.com

InTech China
Unit 405, Office Block, Hotel Equatorial Shanghai
No.65, Yan An Road (West), Shanghai, 200040, China
中国上海市延安西路65号上海国际贵都大饭店办公楼405单元
Phone: +86-21-62489820
Fax: +86-21-62489821